GMR
The Original

CORRELATION BETWEEN LABORATORY MARKERS, CT, AND LUNG ULTRASOUND IN COVID-19-POSITIVE CANCER PATIENTS

Salma Zanaty Komy[1], Ahmed Hassan Othman[2], Fatma Adel Diab[3], Mohamed M. El Barody[4], Mohamed Farouk Mohamed[5], Eman Mosaad Zaki[6], Rania Mohamed Abdelemam[7]

[1.] Assistant Lecturer, Department of Anesthesia, ICU and Pain Relief, South Egypt Cancer Institute, Asyut University,salma_komy@aun.edu.eg
[2.] Professor, Department of Anesthesia, ICU and Pain Relief, South Egypt Cancer Institute, Asyut University, Ahmadhothman@aun.edu.eg
[3.] Professor, Department of Anesthesia, ICU and Pain Relief, South Egypt Cancer Institute, Asyut University, fatma_anethesia@aun.edu.eg
[4.] Associate Professor, Department of Radio Diagnosis, South Egypt Cancer Institute, Asyut University, elbarody_radiol@yahoo.com
[5.] Associate Professor, Department of Anesthesia, ICU and Pain Management, South Egypt Cancer Institute, Asyut University, mfaroukma@aun.edu.eg
[6.] Professor, Department of Clinical Pathology, South Egypt Cancer Institute, Asyut University, eman_mosaad@aun.edu.eg
[7.] Associate Professor, Department of Anesthesia, ICU and Pain Management, South Egypt Cancer Institute, Asyut University, rania-20002@aun.edu.eg

ABSTRACT

Background: Imaging of the chest is an essential tool for assessing the course of a disease. The purpose of this study was to examine lung ultrasound (LUS) and chest CT in cancer patients with mild to severe COVID-19 pneumonia, in addition to clinical traits and test indicators such as serum ferritin, D-dimer, interleukin-6 (IL-6), and C-reactive protein (CRP).

Methods: This cohort validation study included 30 adult cancer patients (>18 years) of both sexes, From January 2022 until December 2023, they were admitted to the South Egypt Cancer Institute at Assiut University in Egypt due of proven COVID-19 pneumonia.

Diagnosis was confirmed by PCR of nasopharyngeal samples. All patients had CO-RADS 4 or 5 and moderate to severe symptoms. Chest CT was performed prior to admission, and LUS was done within 24 hours of ICU admission. Follow-up was conducted after two weeks. D-dimer, CRP, ferritin, and IL-6 levels were evaluated at baseline and at follow-up.

Results: Significant reductions were observed in pulmonary nodules, lymphadenopathy, and bronchiectasis ($P < 0.05$). CO-RADS categories improved significantly ($P = 0.021$). LUS scores at baseline were significantly higher than total severity scores (TSS) ($P = 0.031$), persisting at follow-up ($P = 0.029$). CRP levels decreased significantly from 38.97 ± 5.7 mg/ml to 27.6 ± 3.7 mg/ml ($P = 0.010$).

Conclusions: LUS is a dependable imaging technique for determining lung involvement. It provides a valuable, non-invasive bedside tool that complements CT findings and laboratory biomarkers for monitoring disease progression and patient management outcomes in clinical practice settings.

KEYWORDS: Chest CT; Lung Ultrasound; D-Dimer; Interleukin-6; Ferritin; C-Reactive Protein

INTRODUCTION

The risk of contracting coronavirus disease 2019 (COVID-19) is dramatically increased for cancer patients. They exhibit greater susceptibility than individuals without cancer [1].

COVID-19 is a viral disease caused by the novel severe acute respiratory syndrome coronavirus 2 (SARS-CoV-2), affecting the respiratory system and other organs that express the ACE2 receptor. It is optimised for fast transmission throughout the respiratory tract by droplets, respiratory secretions, and direct contact [2].

Infections caused by SARS-CoV-2 are primarily transmitted through respiratory particles. The ACE2 receptors present on human respiratory epithelial cells facilitate the entry of SARS-CoV-2 into host cells [3].

The processes by which the cancer-associated condition affects the mortality rate from COVID-19 remain ambiguous. Older adults and persons with comorbidities (including diabetes mellitus, cardiovascular disease, pulmonary illness, hyperlipidaemia, obesity, and chronic kidney and liver disease) may demonstrate heightened susceptibility to severe infections [3].

In patients who are admitted to the hospital with fever or respiratory symptoms, chest X-ray (CXR) or computed tomography (CT) imaging is an essential component of the COVID-19 diagnosis [4].

Chest CT may aid in the diagnosis, detection of complications, and prognostication of COVID-19. Nevertheless, chest CT examinations may produce both false-negative and false-positive results [5].

A diagnostic tool that is broadly accessible and can provide a significant amount of diagnostic information in a variety of respiratory diseases is bedside lung ultrasound (LUS) [6].

Considering the pathophysiology of severe COVID-19, characterised by a hyperinflammatory state, coagulation cascade activation, and multiorgan dysfunction, various biomarkers including CRP, procalcitonin (PCT), erythrocyte sedimentation rate (ESR), IL-6, D-dimer, LDH, and albumin may be pivotal in forecasting COVID-19 results [7].

A dysregulated immune response is produced as a result of severe SARS-CoV-2 infection, which contributes to the pathogenesis by overproducing inflammatory cytokines and chemokines. The initial immune responses' viral evasion and the subsequent immunological misfiring, which results in collateral tissue injury in infected organs, are significant factors in severe COVID-19 [8].
The objective of this investigation was to evaluate the CT and LUS findings in cancer patients who were admitted to the ICU and had moderate or severe COVID-19 viral pneumonia. The results were associated with the laboratory data, which encompassed the levels of IL-6, D-dimer, serum ferritin, and CRP in cancer patients during the quarantine period.

MATERIALS AND METHODS

This observational cohort validation study included 30 individuals aged over 18, of both genders, diagnosed with COVID-19 viral pneumonia, with CT scan Chest findings of CORAD 4 and 5, with moderate to extreme symptoms, validated by PCR from a nasopharyngeal swab.
The research was conducted from January 2022 to December 2023 with approval from the Ethical Committee of the Egypt Cancer Institute (SECI), Assiut University, Assiut, Egypt. Permission to carry out this study came from the Institutional Ethical Committee and registration on clinicaltrials.gov (ID NCT05279378), and the study status is complete. Consent after full explanation was obtained from participants or their families. Obtaining ethical approval from the Institutional Review Board of the South Egypt Cancer Institute, Assiut University (SECI-IRB: IORG 0006563).
Hepatic and renal disorders, coagulopathy, and severe cardiorespiratory conditions unrelated to COVID-19 viral pneumonia were classified as exclusionary criteria.
All patients received radiological assessments, comprising chest CT and lung ultrasound, alongside standard laboratory tests and particular biomarkers including D-dimer, serum ferritin, CRP, and IL-6.
The research was structured as a prospective observational study with a double-blinded assessment. Radiologists interpreting chest CT images were blinded to the LUS findings, while investigators performing LUS assessments were blinded to the CT results, in order to minimize inter-modality assessment bias.
A chest CT scan was obtained before admission, and LUS was performed within 24 hours of ICU admission at the same center. Patients were subsequently followed up two weeks after admission.
To examine the dynamic alterations in D-dimer, CRP, serum ferritin, and IL-6 levels in COVID-19 viral pneumonia, blood samples were collected from each cancer patient at admission and two weeks later, correlating these values with the patient's clinical condition.
The radiologists analysing chest CT and LUS results were unaware of the patients' clinical and laboratory information. The investigators doing laboratory measurements were blinded to the radiological findings and clinical outcomes to reduce potential assessment bias.

Computed tomography technique

As part of the evaluation process for suspected COVID-19 viral pneumonia, all cancer patients who were part of the trial had CT scans right before being admitted. Using a GE LightSpeed 16-slice scanner, CT imaging was performed. The CT severity score was determined by an expert radiologist who analysed the images, taking into account the distribution and magnitude of GGOs and consolidations.
The COVID-19 Reporting and Data System score (CO-RADS) is dependent on the degree of suspicion of pulmonary involvement in COVID-19 viral pneumonia, was used to classify CT scans [9]. All CT scans were performed in the supine position at end-inspiration without the use of intravenous contrast.
A proficient radiologist evaluated the CT images to detect and quantify thoracic anomalies, including assessing the degree of ground-glass opacities and consolidations using a grading system **(Figure 4)**. A score was assigned to each lung lobe based on the percentage of involvement. [Score 0: 0% involvement; Score 1: less than 5% involvement; Score 2: 5% to less than 25% involvement; Score 3: 25% to less than 50% involvement; Score 4: 50% to less than 75% involvement; Score 5: 75% or more involvement].
The combined CT scores of the right and left lungs provided a semi-quantitative evaluation of the overall severity score, with a maximum of 25 for both lungs.
The categorisation of disease severity according to the percentage of total lung involvement was as follows: None: 0.0%, minimal: 1-25%, mild: 26-50%, moderate: 51-75%, and severe: greater than 76-100%. The Total Severity Score (TSS) and grade were computed for each patient. The TSS threshold for distinguishing severe-critical kinds is 7.5, exhibiting 82.6% sensitivity and 100% specificity [10].

Ultrasound Procedures

Bedside lung ultrasound (LUS) was performed by a clinician uninformed of the CT results within 24 hours of admission and CT assessment. Operators implemented suitable personal protective equipment. A portable ultrasound equipment (Viamo C100, Toshiba) equipped with convex (3.5–5 MHz) and linear (4–8 MHz) probes was employed for COVID-19 patients. Protective coverings were employed for both the probes and the ultrasound machine console during the examination.
Patients were evaluated in a seated position, and a comprehensive examination of the anterior, lateral, and posterior chest walls of both haemithoraces was conducted. A convex transducer was employed to view the pleural line and lung

parenchymal artefacts, including A-lines, B-lines, and consolidation. The pleural line and subpleural anomalies were later evaluated in depth with a linear probe.
The anterior, lateral, and posterior regions of each haemithorax were delineated. Regarding the anterior sector: situated between the parasternal line and the anterior axillary line. Lateral sector: situated between the anterior and posterior axillary lines. Posterior sector: situated between the posterior axillary line and the paravertebral line.
Each sector was divided into superior and inferior halves, utilising the third intercostal space as a reference to delineate sections for each haemithorax. Images were archived using the ultrasound software and subsequently evaluated by operators after the examination to minimise prolonged patient engagement.
Each of the 12 anatomical sites was assigned a score from 0 to 3 according to the ultrasonography scoring system: 0 indicates a normal pleural line with A lines; 1 denotes an indented pleural line with focal B lines; 2 signifies a disrupted pleural line with subpleural consolidations; and 3 represents a white lung, with or without consolidations [11]. The result of each score, together with the specifics of each zone, was documented in a table and retained in the patient's medical record. Upon conclusion of the procedure, the doctor documented the maximum score achieved for each area [12].

Clinical Data
Essential parameters (heart rate, mean arterial pressure, temperature, and oxygen saturation) were continually observed. Clinical data was recorded on admission, including malignancy type, symptom occurrence, comorbidities, and COVID-19 severity. Additional investigations, D-dimer, CRP, IL-6, and serum ferritin, were documented on admission and after 2 weeks.

Sample processing
Blood samples were collected aseptically to assess inflammatory and coagulation biomarkers, with laboratory staff blinded to participants' clinical data. Serum was used to measure CRP and IL-6, while citrate-anticoagulated plasma was collected for D-dimer analysis. CRP and D-dimer were determined by turbidimetric methods, and IL-6 by ELISA. Samples were processed using normal procedures, kept on ice, and centrifuged at 2000g for 20 minutes at 4 °C within 30 minutes of collection. Plasma was preserved at −80 °C in aliquots and thawed just once before analysis.
The primary objective was to investigate the results of CT and LUS in cancer patients who were admitted to the ICU with mild to severe COVID-19 viral pneumonia and to establish a correlation between these findings and clinical characteristics. The secondary outcomes aimed to link the findings with clinical and laboratory data, including levels of IL-6, D-dimer, serum ferritin, and CRP in cancer patients during the quarantine period.

Quantitative analysis
Statistical analysis was performed utilising SPSS version 26 (IBM Inc., Chicago, IL, USA). Quantitative data were presented as mean and standard deviation (SD) and analysed between the two groups using an unpaired Student's t-test. Qualitative variables were expressed as frequencies and percentages and examined using the Chi-square test or Fisher's exact test as appropriate. A two-tailed P value below 0.05 was considered statistically significant.

RESULTS
Sixty-four patients were evaluated for eligibility. Six patients were excluded, consisting of four who did not satisfy the inclusion criteria and two who opted out of participation. As a result, 58 patients were recruited for the study. During the follow-up period, 28 patients were unaccounted for, comprising 19 fatalities and nine owing to missed follow-up appointments. Ultimately, data from thirty patients were incorporated into the final analysis. **(Figure 1)**
Sociodemographic and clinical characteristics were enumerated in **Table 1**.
There were insignificant differences in LUS findings between baseline and follow-up, i.e., Compound B lines (<50%), Compound B lines (>50%), consolidation, Air-bronchogram, pleural effusion, and pleural thickening. For the total LUS score, there was an insignificant difference in follow-up vs. baseline. (**Table 2)**
The follow-up results for bilateral or unilateral multifocal ground-glass opacities (GGO) did not show significant differences in consolidation pattern, crazy paving, pleural effusion, tree-in-bud sign, pleural thickening, fibrosis, pneumothorax, or TSS score as compared to baseline. Significant reductions were observed in lung nodules (3.3% vs. 33.3%, P = 0.003), lymphadenopathy (0% vs. 30%, P = 0.002), and bronchiectasis (0% vs. 20%, P = 0.003). At follow-up, five seriously sick individuals (16.7%) demonstrated recovery from baseline. Furthermore, a notable enhancement in the CORADS category was observed during follow-up (P = 0.021). (**Table 3)**
The baseline LUS score was substantially greater than the TSS score (P = 0.031). Likewise, the LUS score at follow-up was markedly elevated compared to the TSS score (P = 0.029). Furthermore, there was a notable reduction in CRP levels from 38.97 ± 5.7 mg/ml at baseline to 27.6 ± 3.7 mg/ml at follow-up (P = 0.010). Conversely, little variations were noted in the means of D-dimer, serum ferritin, and IL-6. (**Table 4)**

DISCUSSION
Pneumonia is widely prevalent worldwide, while viral pneumonia constitutes a common cause of hospitalization. Moreover, viral pneumonia increases both the risk and severity of bacterial pneumonia and is associated with co-infection [13].

Regarding LUS, there were insignificant changes in the findings between baseline and follow-up, i.e., compound B lines (<50%), compound B lines (>50%) (**Figure 2)**, consolidation, air-bronchogram, pleural effusion (**Figure 3),** and pleural thickening. For the total LUS score, there was an insignificant decrease in follow-up (16.8 ± 2.1) vs baseline.

Consistent with our research, Raiteri et al. [14] determined that LUS possesses a high prevalence of mild abnormalities in healthy individuals and limited sensitivity in asymptomatic cases. Minor abnormalities such as isolated B-lines or minimal pleural irregularities may occasionally be detected without pathological significance. In the same context, Volpicelli and Gargani [15] emphasized that, although individual sonographic signs are not specific on their own, combining them into recognized patterns and correlating them with clinical and laboratory findings enhances the diagnostic power of LUS.

LUS demonstrated high sensitivity for SARS-CoV-2 pneumonia, particularly in moderate to severe cases, though specificity was limited because findings may overlap with other interstitial lung diseases. Serial LUS examinations were valuable for assessing disease progression and treatment response. Unlike our study, Trias-Sabrià et al. [16] found that LUS scores (≥24 points) experienced ICU admission or death in a study done on 36 participants with a 30 day follow-up period after admission.

In our cohort, the diminished mean cutoff value (16.93 points at baseline, 16.77 points at follow-up) may be attributed to the high-risk profile of the cohort, as the participants were oncology cases with numerous associated risk factors. Moreover, Sperandeo et al. [17], in comparative studies evaluating LUS versus CXR for pediatric pneumonia diagnosis, typically enrolled children with clinical suspicion of pneumonia aged from infancy to adolescence. Each child underwent both imaging modalities (LUS and CXR) after clinical assessment. The quantity and distribution of ground-glass opacities and consolidations in chest CT scans were thoroughly evaluated by skilled radiologists.

The results suggested that all patients revealed CT abnormalities consistent with bilateral COVID-19 pneumonia, whereas LUS revealed distinctive patterns, including localised and confluent B lines, subpleural microconsolidations, and larger parenchymal consolidations. The LUS score demonstrated a significant correlation with CT visual scoring ($p < 0.001$) and with oxygen saturation in ambient air, indicating that LUS effectively reflects the severity of pulmonary involvement seen on CT and supports its use as a dependable diagnostic instrument in suspected COVID-19 pneumonia.

Similarly, Deif et al. [18] found that subpleural consolidation in 38.46% of patients and effusion in 12.31% of patients. A CT chest showed pleural thickening in 33.85% of patients. Nouvenne et al. [19] identified a substantial correlation between LUS scores and CT visual ratings, demonstrating that LUS accurately represents the degree and pattern of pulmonary involvement observed on CT.

In our results, regarding multifocal GGO, there was insignificant change in the rate of both bilateral and unilateral multifocal GGO at follow-up in comparison with baseline. Likewise, there was insignificant change in the rate of consolidation, predominant pattern, Crazy paving pattern, pleural effusion and Tree-in-bud sign at follow-up than baseline, indicating persistence of specific lung patterns. However, for the CORADS, there was significant improvement in CORADS category at follow-up compared to baseline. As the CORADS category suggests, overall radiological recovery and a decrease in disease severity are expected.

This indicates that global CT evaluation may more accurately represent clinical improvement than specific lesion patterns in oncology patients afflicted with COVID-19. Prokop et al. [20] claimed that the CO-RADS, a categorical assessment approach for assessing pulmonary involvement in COVID-19 with unenhanced chest CT, has shown strong interobserver agreement and good efficacy in predicting COVID-19 in patients with moderate to severe symptoms .

Our study demonstrated substantial decreases at follow-up in pulmonary nodules (3.3% vs. 33.3%, $p = 0.003$), lymphadenopathy (0% vs. 30%, $p = 0.002$), and bronchiectasis (0% vs. 20%, $p = 0.003$), whereas pleural thickening, fibrosis, pneumothorax, and mean TSS score (13.1 ± 3.5 at baseline) exhibited no significant changes. Five critically ill patients (16.7%) recovered at follow-up. These findings suggest resolution of acute inflammatory CT changes associated with COVID-19, whereas persistent pleural and fibrotic changes likely reflect more chronic structural involvement, indicating a dissociation between focal radiologic improvement and overall severity scores. According to Luger et al. [21], A decrease in CT severity score was noted in participants during the subsequent follow-up CT.

In concordance with our findings, Gurumurthy et al. [22] verified that the low incidence of pulmonary nodules was 4.3%. In our study, the prevalence of hilar lymphadenopathy was 0.6%. Furthermore, Garg et al. [23] demonstrated the low incidence of bronchiectasis.

In the current study, the LUS score at baseline was significantly higher than the TSS score. Similarly, the LUS score at follow-up was significantly higher than the TSS score. This was supported by Chrzan et al. [24], who reported that a substantial association existed between LUS scores and CT severity scores in patients with COVID-19, supporting the idea that LUS can reflect disease extent comparably to CT. Consistent with our findings, Ciurba et al. [25] demonstrated that LUS is a non-invasive, efficient, and pragmatic tool for the diagnosis, monitoring, and prognostic assessment of COVID-19 patients.

These results correspond with the findings of Portale et al. [26], who identified a robust link between the LUS and CT scores. Elevated scores were correlated with heightened CRP levels.

Therefore, LUS reliably reflects the extent of pulmonary abnormalities detected on CT. These findings support the integration of LUS into clinical practice for early diagnosis and monitoring when combined with clinical and laboratory data, particularly in resource-constrained environments.

Additionally, there was significant reduction in the level of CRP from 38.97 ± 5.7 mg/ml at baseline to 27.6 ± 3.7 mg/ml at follow-up. On the other hand, insignificant differences were observed for the mean of D-dimer, serum ferritin and IL-6, suggesting these markers were less responsive to short-term disease progression in this cohort.
In addition, Velavan et al. [27] found that hospitalised individuals had a substantial reduction in CRP levels from admission to recovery. A notable discrepancy in ferritin levels was detected between hospitalised and ambulatory patients. D-dimer levels upon admission were markedly elevated in hospitalised patients relative to ambulatory patients.
The study's imperfections were a relatively small sample size. The study was performed in a singular location. The patient follow-up was limited to a relatively short period. Dependence on RCR for diagnosis may have diminished the sample size, as several clinically suspected patients with negative PCR findings were omitted. The study did not include a comparison with a healthy control group.

CONCLUSIONS

In cancer patients experiencing moderate to severe COVID-19, lung ultrasound (LUS) serves as a sensitive and dependable instrument for assessing pulmonary involvement. Over a 14-day follow-up, most LUS and CT parameters remained stable, while significant improvements were observed in pulmonary nodules, lymphadenopathy, and bronchiectasis. CORADS categories and CRP levels also showed significant recovery, reflecting partial clinical improvement. LUS is a valuable, non-invasive imaging modality for tracking disease progression and response to therapy in high-risk COVID-19 patients, complementing CT imaging and clinical biomarkers.

REFERENCES

1. Liang W, Guan W, Chen R, Wang W, Li J, Xu K, et al. Cancer patients in SARS-CoV-2 infection: a nationwide analysis in China. Lancet Oncol. 2020;21:335-7.
2. Li Q, Guan X, Wu P, Wang X, Zhou L, Tong Y, et al. Early transmission dynamics in wuhan, china, of novel coronavirus-infected pneumonia. N Engl J Med. 2020;382:1199-207.
3. Datta PK, Liu F, Fischer T, Rappaport J, Qin X. SARS-CoV-2 pandemic and research gaps: Understanding SARS-CoV-2 interaction with the ACE2 receptor and implications for therapy. Theranostics. 2020;10:7448-64.
4. Guan WJ, Ni ZY, Hu Y, Liang WH, Ou CQ, He JX, et al. Clinical characteristics of coronavirus disease 2019 in China. N Engl J Med. 2020;382:1708-20.
5. Kwee TC, Kwee RM. Chest CT in COVID-19: What the Radiologist Needs to Know. Radiographics. 2020;40:1848-65.
6. Luo J, Rizvi H, Preeshagul IR, Egger JV, Hoyos D, Bandlamudi C, et al. COVID-19 in patients with lung cancer. Ann Oncol. 2020;31:1386-96.
7. Upadhyay J, Tiwari N, Ansari MN. Role of inflammatory markers in corona virus disease (COVID-19) patients: A review. Exp Biol Med (Maywood). 2020;245:1368-75.
8. Hariyanto TI, Japar KV, Kwenandar F, Damay V, Siregar JI, Lugito NPH, et al. Inflammatory and haematologic markers as predictors of severe outcomes in COVID-19 infection: A systematic review and meta-analysis. Am J Emerg Med. 2021;41:110-9.
9. Patrucco F, Albera C, Bellocchia M, Foci V, Gavelli F, Castello LM, et al. SARS-CoV-2 Detection on Bronchoalveolar Lavage: An Italian Multicenter experience. Respiration. 2020;99:970-8.
10. Wasilewski PG, Mruk B, Mazur S, Poltorak-Szymczak G, Sklinda K, Walecki J. COVID-19 severity scoring systems in radiological imaging - a review. Pol J Radiol. 2020;85:e361-e8.
11. Falster C, Jacobsen N, Wulff Madsen L, Dahlerup Rasmussen L, Davidsen JR, Christie Knudtzen F, et al. Lung ultrasound may be a valuable aid in decision making for patients admitted with COVID-19 disease. Eur Clin Respir J. 2021;8:190-200.
12. Soldati G, Smargiassi A, Inchingolo R, Buonsenso D, Perrone T, Briganti DF, et al. Proposal for International Standardization of the Use of Lung Ultrasound for Patients With COVID-19: A Simple, Quantitative, Reproducible Method. J Ultrasound Med. 2020;39:1413-9.
13. Ruuskanen O, Luoto R, Valtonen M, Heinonen OJ, Waris M. Respiratory viral infections in athletes: Many unanswered questions. Sports Med. 2022;52:2013-21.
14. Raiteri A, Alvisi M, Serio I, Stefanini F, Tovoli F, Piscaglia F. Lung ultrasound is often, but not always, normal in healthy subjects: Considerations for COVID-19 pandemic. Diagnostics (Basel). 2021;11:12-23.
15. Volpicelli G, Gargani L. Sonographic signs and patterns of COVID-19 pneumonia. Ultrasound J. 2020;12:22-55.
16. Trias-Sabrià P, Molina-Molina M, Aso S, Argudo MH, Diez-Ferrer M, Sabater J, et al. Lung ultrasound score to predict outcomes in COVID-19. Respir Care. 2021;66:1263-70.
17. Sperandeo M, Tinti MG, Rea G. Chest ultrasound versus chest X-rays for detecting pneumonia in children: Why compare them each other if together can improve the diagnosis? Eur J Radiol. 2017;93:291-2.
18. Deif RH, Ibrahim IS, El Heniedy MA, El Shafey MH, Abo Elnasr RM. Correlation between lung ultrasound and chest CT in COVID-19 pneumonia patients on hospital admission. Egypt J Intensive Care Emerg Med. 2025;5:43-58.
19. Nouvenne A, Zani MD, Milanese G, Parise A, Baciarello M, Bignami EG, et al. Lung ultrasound in COVID-19 pneumonia: correlations with chest CT on hospital admission. Respiration. 2020;99:617-24.

20. Prokop M, Van Everdingen W, van Rees Vellinga T, Quarles van Ufford H, Stöger L, Beenen L, et al. CO-RADS: a categorical CT assessment scheme for patients suspected of having COVID-19—definition and evaluation. Radiol. 2020;296:97-104.
21. Luger AK, Sonnweber T, Gruber L, Schwabl C, Cima K, Tymoszuk P, et al. Chest CT of lung injury 1 year after COVID-19 pneumonia: the CovILD study. Radiol. 2022;304:462-70.
22. Gurumurthy B, Das SK, Hiremath R, Shetty S, Hiremath A, Gowda T. Spectrum of atypical pulmonary manifestations of COVID-19 on computed tomography. Egypt J Radiol Nucl Med. 2021;52:72-55.
23. Garg M, Prabhakar N, Bhatia H, Dhooria S, Debi U, Muthu V, et al. CT findings in sequel of COVID-19 pneumonia and its complications. BJR| Open. 2021;3:202-50.
24. Chrzan R, Polok K, Antczak J, Siwiec-Koźlik A, Jagiełło W, Popiela T. The value of lung ultrasound in COVID-19 pneumonia, verified by high resolution computed tomography assessed by artificial intelligence. BMC Infect Dis. 2023;23:195-200.
25. Ciurba BE, Sárközi HK, Szabó IA, Ianoși ES, Grigorescu BL, Csipor-Fodor A, et al. Applicability of lung ultrasound in the assessment of COVID-19 pneumonia: Diagnostic accuracy and clinical correlations. Respir Investig. 2022;60:762-71.
26. Portale G, Ciolina F, Arcari L, Giraldi GDL, Danti M, Pietropaolo L, et al. Lung ultrasound in COVID-19: clinical correlates and comparison with chest computed tomography. SN Compr Clin Med. 2021;3:2075-81.
27. Velavan TP, Kuk S, Linh LTK, Lamsfus Calle C, Lalremruata A, Pallerla SR, et al. Longitudinal monitoring of laboratory markers characterizes hospitalized and ambulatory COVID-19 patients. Sci Rep. 2021;11:144-50.

List of figures:

Figure 1: CONSORT flow chart of the enrolled patients

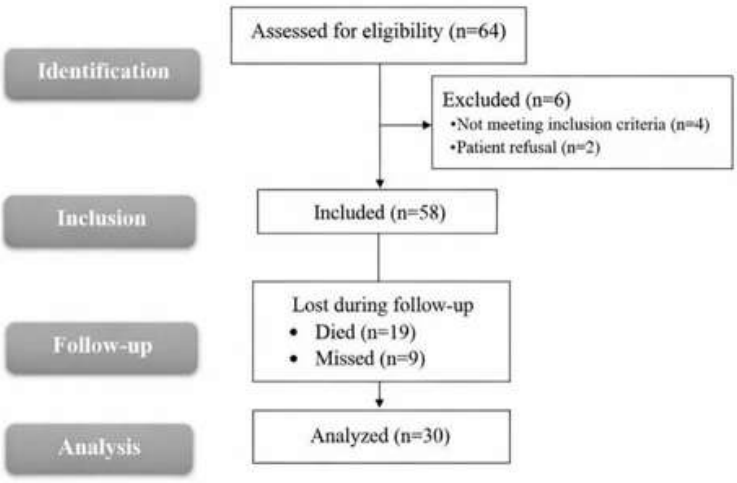

Figure 2: **Lung ultrasound images showing B-lines (comma-tail artifacts) by using a convex probe**

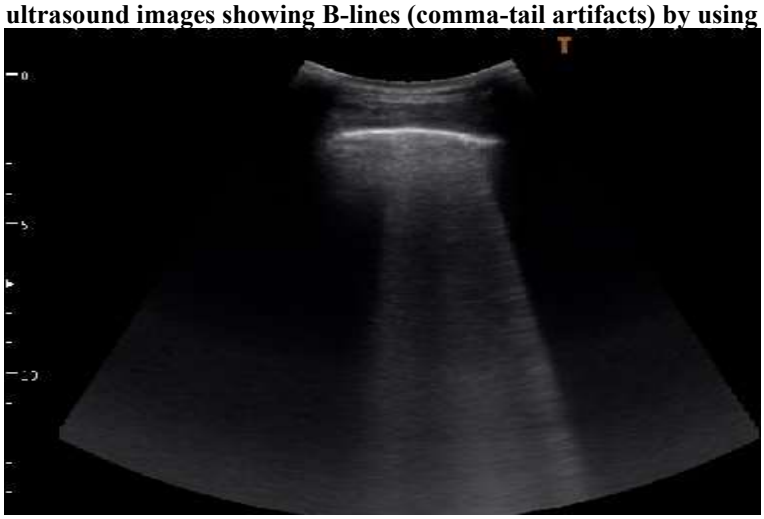

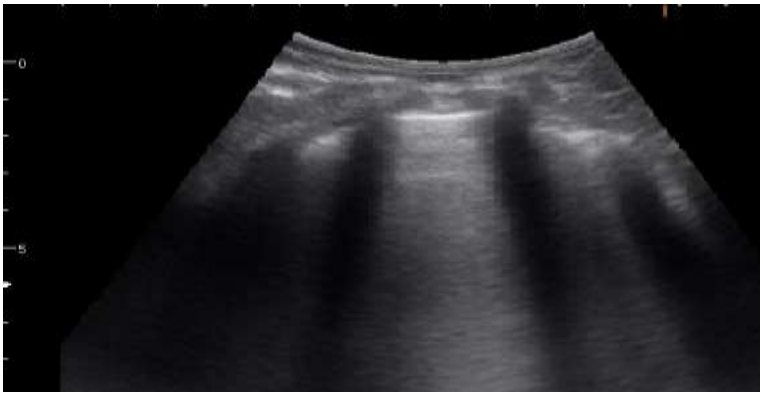

Figure 3: **Lung ultrasound images showing lung consolidation with air bronchogram and pleural effusion**

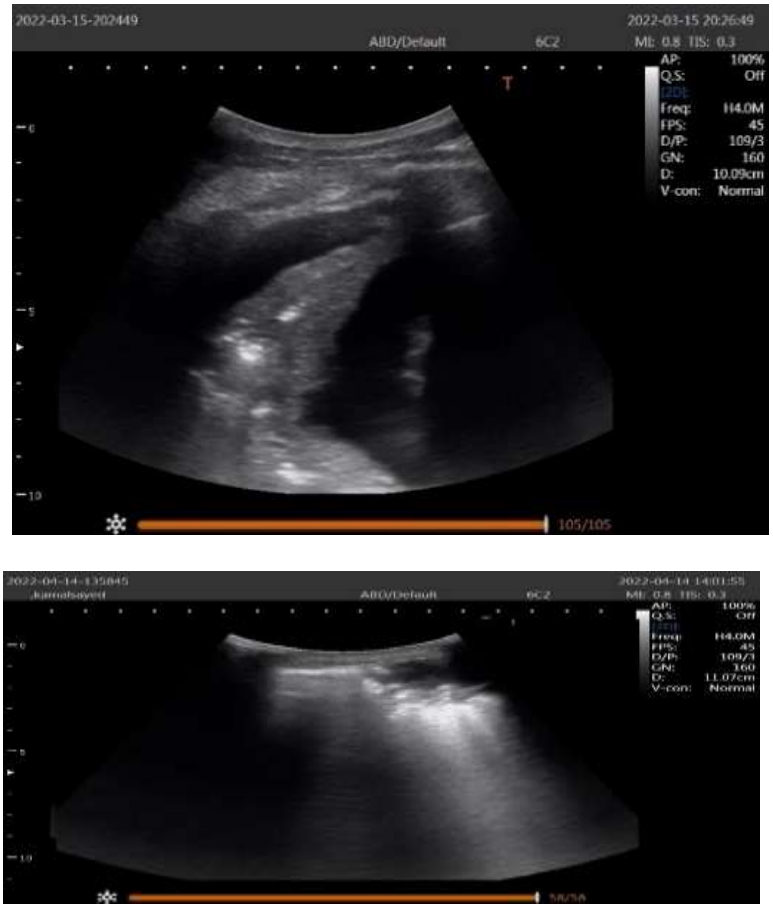

Figure 4: CT image showing pulmonary window of bilateral multi-focal ground glass densities seen at both lung fields and bilateral mild pleural (4a), CT image showing pulmonary window of Bilateral multi-focal ground glass densities seen at right lung fields (4b)

4a

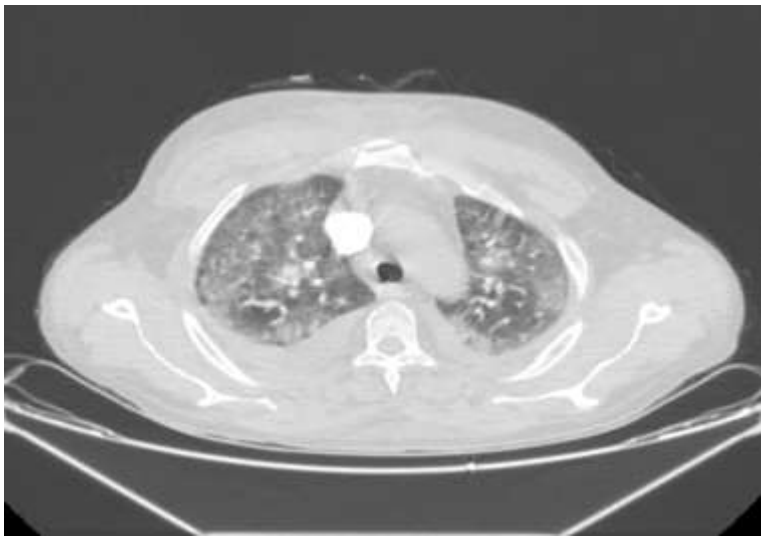

(4b)

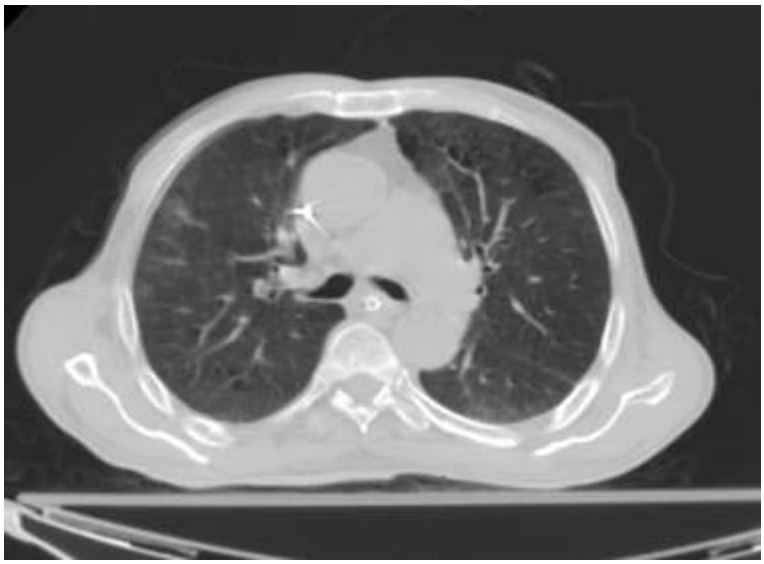

List of tables:

Table 1: Sociodemographic and clinical characteristics of the cohort study

		N=30
Age (Years)		47.37 ± 13.2
Sex	**Male**	19(63.3%)
	Female	11(36.7%)
Smoking Status	**Smoker**	8 (26.7%)
Oxygenation	**Vent. 40%**	7 (23.3%)
	Vent. 50%	17 (56.7%)
	Vent. 60%	6 (20%)
MV		8 (26.7%)
Type of Malignancy	**Upper GIT**	7 (23.3%)
	Lower GIT	4 (13.3%)
	Leukaemia	5 (16.7%)
	Lymphoma	5 (16.7%)
	Organ	8 (26.7%)
	MM	1 (3.3%)

CORAD	**CORAD-IV**	9 (30%)
	CORAD-V	21 (70%)
Symptoms	**Fever**	16 (53.3%)
	Cough	28 (93.3%)
Comorbidity	**DM**	2 (6.7%)
	HTN	2 (6.7%)

Data are presented as mean ± SD or frequency. MV: Mechanical ventilation, GIT: Gastrointestinal tract, MM: Multiple Myeloma, CORAD: COVID-19 Reporting and Data System, DM: Diabetes mellitus, HTN: Hypertension.

Table 2: Differences in Chest U/S Parameters after 14 days from admission

	Baseline (n=30)	**FU (n=30)**	**P**
Compound B lines (<50%)	12 (40%)	15 (50%)	0.426
Compound B lines (>50%)	17 (65.7%)	15 (50%)	0.605
Consolidation	18 (60%)	19 (63.3%)	0.791
Air Bronchogram	5 (16.7%)	8 (26.7%)	0.347
Pleural Effusion	23 (76.7%)	23 (76.7%)	1.000
Pleural Thickening	11 (36.7%)	12 (40%)	0.791
LUS	17.80 ± 1.7	16.77 ± 2.1	0.504

Data are presented as mean ± SD or frequency. The McNemar test was used to compare the differences in Frequency over time within the group. US: Ultrasound, FU: Follow up, LUS: Lung ultrasound.

Table 3: Differences in CT findings and CORAD score on admission and after 14 days

		Baseline (n=30)	**FU (n=30)**	**P**
Multi-focal GGO	**Bilateral**	20 (66.7%)	24 (80%)	0.243
	Unilateral	9 (30%)	4 (13.3%)	0.117
Consolidation		23 (39.7%)	8 (13.8%)	0.118
Crazy paving pattern		1 (3.3%)	0 (0%)	0.627
Atypical findings	**Pleural effusion**	24 (80%)	25 (83.3%)	0.739
	Pulmonary nodules	10 (33.3%)	1 (3.3%)	**0.003***
	Lymphadenopathy	9 (30%)	0 (0%)	**0.002***
	Tree-in-bud sign	4 (13.3%)	1 (3.3%)	0.353
	Bronchiectasis	6 (20%)	0 (0%)	**0.024***
	Isolated pleural thickening	9 (30%)	6 (20%)	0.552
	Pulmonary fibrosis	5 (16.7%)	1 (3.3%)	0.195
	Pneumothorax	0 (0%)	0 (0%)	-----
	TSS	13.03 ± 3.5	12.60 ± 5.5	0.683
TSS Category	**Severe-Critical (TSS>7.5)**	28 (93.3%)	23 (76.7%)	0.146
CORADS	**CORADS-II**	1 (3.3%)	3 (3.3%)	**0.021***
	CORADS-III	0 (0%)	3 (3.3%)	
	CORADS-VI	8 (26.7%)	6 (20%)	
	CORADS-V	21 (70%)	18 (60%)	

Data are presented as mean ± SD or frequency (%). * Significant P value < 0.05, the McNemar test was used to compare the differences in Frequency over time within the group. Paired Sample t-test was used to compare the differences in Mean over time within the group, CT: Computed tomography, FU: Follow up, CORAD: COVID-19 Reporting and Data System, LUS: Lung ultrasound, GGO: Ground glass opacities, TSS: Total severity score.

Table 4: Differences in TSS, LUS and disease biomarkers over 14 days

	Baseline (n=30)	**FU (n=30)**	**P**
LUS score	16.93 ± 1.7	16.77 ± 2.1	0.504
TSS score	13.03 ± 3.5	12.60 ± 5.5	0.683
P-value	**0.031***	**0.029***	
Disease Biomarkers			
D-Dimer (µg/mL)	2.33 ± 0.3	2.22 ± 0.2	0.514
S. Ferritin (ng/ml)	1674.40 ± 316.2	1265.90 ± 128.3	0.156
IL-6 (pg/ml)	0.15 ± 0.02	0.14 ± 0.02	0.316
CRP (mg/dL)	38.97 ± 5.7	27.63 ± 3.7	**0.010***

Data are presented as mean ± SD. * Significant P value < 0.05, Paired Sample t-test was used to compare the differences in means over time within group, Independent Sample t-test was used to compare the differences in Means, LUS: Lung ultrasound, TSS: Total severity score, IL-6: Interleukin-6, CRP: C-reactive protein.